

Article

Fluorinated Analogs of Organosulfur Compounds from Garlic (*Allium sativum*): Synthesis, Chemistry and Anti-Angiogenesis and Antithrombotic Studies

Eric Block ^{1,*} , Benjamin Bechand ¹, Sivaji Gundala ¹, Abith Vattekkatte ¹, Kai Wang ¹, Shaymaa S. Mousa ², Kavitha Godugu ², Murat Yalcin ^{2,3} and Shaker A. Mousa ^{2,*} 

¹ Department of Chemistry, University at Albany, State University of New York, Albany, NY 12222, USA; bb2858@columbia.edu (B.B.); Sivaji.Gundala@amriglobal.com (S.G.); avattekkatte@ice.mpg.de (A.V.); kwang40@its.jnj.com (K.W.)

² The Pharmaceutical Research Institute, Albany College of Pharmacy and Health Sciences, Rensselaer, NY 12144, USA; shaymaa.mousa@gmail.com (S.S.M.); Kavitha.Godugu@acphs.edu (K.G.); mrtylcn75@gmail.com (M.Y.)

³ Department of Physiology, Veterinary Medicine Faculty, Uludag University, Bursa 16059, Turkey

* Correspondence: eblock@albany.edu (E.B.); shaker.mousa@acphs.edu (S.A.M.); Tel.: +1-518-442-4459 (E.B.); +1-518-694-7397 (S.A.M.)

Received: 6 October 2017; Accepted: 24 November 2017; Published: 28 November 2017

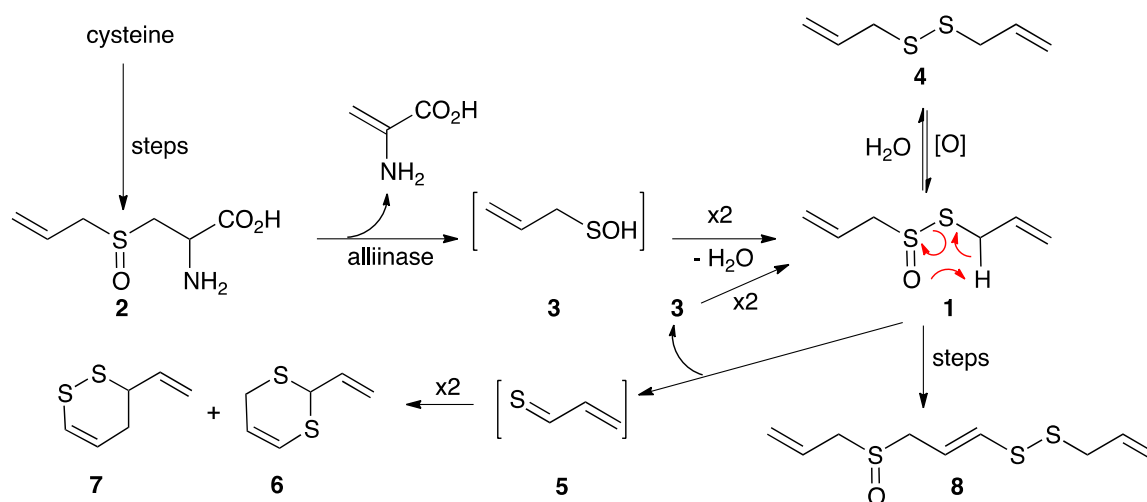
Abstract: We describe the synthesis, reactivity, and antithrombotic and anti-angiogenesis activity of difluoroallicin (*S*-(2-fluoroallyl) 2-fluoroprop-2-ene-1-sulfinothioate) and *S*-2-fluoro-2-propenyl-L-cysteine, both easily prepared from commercially available 3-chloro-2-fluoroprop-1-ene, as well as the synthesis of 1,2-bis(2-fluoroallyl)disulfane, 5-fluoro-3-(1-fluorovinyl)-3,4-dihydro-1,2-dithiin, trifluoroajoene ((*E,Z*)-1-(2-fluoro-3-((2-fluoroallyl)sulfinyl)prop-1-en-1-yl)-2-(2-fluoroallyl)disulfane), and a bis(2-fluoroallyl)polysulfane mixture. All tested organosulfur compounds demonstrated effective inhibition of either FGF or VEG-mediated angiogenesis (anti-angiogenesis activity) in the chick chorioallantoic membrane (CAM) or the mouse Matrigel[®] models. No embryo mortality was observed. Difluoroallicin demonstrated greater inhibition ($p < 0.01$) versus organosulfur compounds tested. Difluoroallicin demonstrated dose-dependent inhibition of angiogenesis in the mouse Matrigel[®] model, with maximal inhibition at 0.01 mg/implant. Allicin and difluoroallicin showed an effective antiplatelet effect in suppressing platelet aggregation compared to other organosulfur compounds tested. In platelet/fibrin clotting (anti-coagulant activity), difluoroallicin showed concentration-dependent inhibition of clot strength compared to allicin and the other organosulfur compounds tested.

Keywords: garlic; allicin; vinyl dithiins; ajoene; difluoroallicin; trifluoroajoene; angiogenesis; anti-angiogenesis; platelet; coagulation; thrombosis; anti-thrombotic; 2-fluoroallyl sulfur compounds

1. Introduction

Since its discovery by Cavallito in 1944, the antibiotic active principle of garlic, allicin (1), has been the subject of extensive research [1–3]. Enzymatically released from its precursor alliin (2) when garlic is crushed, allicin is both unstable and reactive, readily decomposing by way of 2-propenesulfenic acid (3) and thioacrolein (5) to diallyl disulfide (4) and homologous polysulfides (polysulfanes), vinyl 1,2- and 1,3-dithiins (6 and 7, respectively) and ajoene (8) (Scheme 1), among other products, all of which have interesting biological properties, e.g., as antiplatelet and anticancer agents [1–8]. Given the great importance of fluorine in medicinal chemistry and chemical biology [9,10], we were interested in the effect that fluorine substitution would have on the chemical reactivity and biological activity of

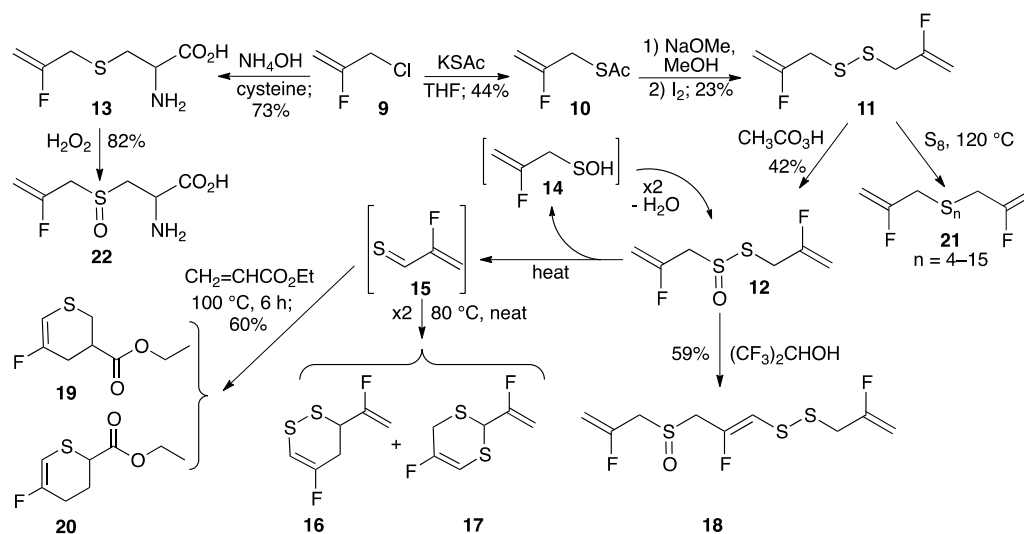
these compounds, since such fluorinated analogs are presently unknown. Compounds with C–F bonds, particularly of the sp^2 -C–F type, offer advantages associated with the small size, high electronegativity, and metabolic stability associated with the fluorine as well as the altered molecular lipophilicity, membrane fluidity, binding affinity, enhanced volatility, and possibilities for halogen bonding [11] and conformational preferences of the fluorinated compounds compared to their hydrogen analogs. We also follow up on our previous work on trifluoroselenomethionine [12]. Thiol group reactivity, a defining feature of the biological activity of allicin and other garlic compounds [13–15], should be enhanced by H/F substitution in garlic thioallyl compounds.



Scheme 1. Enzymatic formation of allicin (1) from alliin (2) by way of 2-propenesulenic acid (3), synthesis of allicin by oxidation of diallyl disulfide (4), conversion of 1 to ajoene (8), and decomposition of 1 to vinyl dithiins (6 and 7) via intramolecular elimination to thioacrolein (5).

Three types of C–F substituted allyl groups were considered for this study, namely $CH_2=CFCH_2-X$ (**A**), $CF_2=CFCH_2-X$ (**B**), and $CF_2=CFCH_2-X$ (**C**). We chose type **A** based on commercial availability of $CH_2=CFCH_2Cl$ (3-chloro-2-fluoroprop-1-ene (**9**)) (Scheme 2), as well as on our inability to convert thioacetate $CF_2=CFCH_2SAc$ (from Mitsunobu reaction of $CF_2=CFCH_2OH$ [16]) to the corresponding disulfide, and on the relative inaccessibility of precursors **C**, such as $CF_2=CFCH_2OSO_2F$ [17]. Here, we describe our efforts to synthesize and study the reactivity and activity of difluoroallicin **12** (*S*-(2-fluoroallyl) 2-fluoroprop-2-ene-1-sulfinothioate), easily prepared from **9**, and related compounds such as *S*-2-fluoro-2-propenyl-L-cysteine (fluorodeoxyalliin, **13**), 1,2-bis(2-fluoroallyl)disulfane (**11**), 5-fluoro-3-(1-fluorovinyl)-3,4-dihydro-1,2-dithiin (**16**), trifluoroajoene ((*E,Z*)-1-(2-fluoro-3-((2-fluoroallyl)sulfinyl)prop-1-en-1-yl)-2-(2-fluoroallyl)disulfane, **18**), and 1,2-bis(2-fluoroallyl)polysulfane (**21**). We also describe the anti-angiogenesis and antithrombotic activity of some of these compounds.

Cancer progression is known to be accelerated by angiogenesis and thrombosis (platelet/fibrin) stimulation, which in turn are mediated by various factors secreted by cancer cells [18–20]. We previously showed that garlic-derived bioactive compounds modulate angiogenesis [5], which might impact cancer progression and suggests potential cancer chemoprevention by organosulfur compounds, as we further examine in this study. Additionally, studies suggest potential platelet function modulation by garlic derived bioactive compounds [21,22]. Our current studies compared the efficacy of fluorinated and non-fluorinated organosulfur compounds on angiogenesis activation by either bFGF or VEGF as well as their comparative efficacy on platelet and coagulation activation.



Scheme 2. Synthesis of difluoroallicin (**12**) from 1-chloro-2-fluoro-2-propene (**9**) by way of thioacetate **10** and bis(2-fluoro-2-propenyl) disulfide (**11**), synthesis of *S*-2-fluoro-2-propenyl-L-cysteine (**13**) from **9**, conversion of **12** to vinyl dithiins **16** and **17** via 2-fluorothioacrolein (**15**) with loss of 2-fluoro-2-propenesulfenic acid (**14**), conversion of **12** to trifluoroajoene **18**, Diels-Alder trapping of **15** with ethyl acrylate giving thiopyrans **19** and **20**, conversion of **11** to polysulfane mixture **21** and conversion of **13** to (+)-*S*-2-fluoro-2-propenyl-L-cysteine *S*-oxide (**22**).

2. Results and Discussion

2.1. Synthesis of Fluorinated Analogues of Garlic-Derived Organosulfur Compounds

It was anticipated that difluoroallicin **12** could be prepared by oxidation of 1,2-bis(2-fluoroallyl)disulfane (**11**), which in turn could be synthesized from commercially available 1-chloro-2-fluoro-2-propene (**9**). Thus, **9** was stirred overnight with potassium thioacetate in THF giving *S*-(2-fluoroallyl) ethanethioate (**10**) in 44% yield. Hydrolysis of **10** (NaOMe/MeOH) followed by treatment with iodine gave **11**. Treatment of a chloroform solution of **11** with peracetic acid gave difluoroallicin **12** (*S*-(2-fluoroallyl) 2-fluoroprop-2-ene-1-sulfinothioate) in 42% yield as a yellow liquid with an onion-like odor. When a chloroform solution of **12** was heated in a sealed tube at 80 °C for 4 h it decomposed giving a mixture of 5-fluoro-3-(1-fluorovinyl)-3,4-dihydro-1,2-dithiin (**16**) as the major product and 5-fluoro-2-(1-fluorovinyl)-4*H*-1,3-dithiin (**17**) as the minor product. If a mixture of **12** and a five-fold excess of ethyl acrylate was heated in a sealed tube at 100 °C for 6 h, a 70:30 mixture of the regioisomeric Diels-Alder adducts (**19** and **20**) of ethyl acrylate and 2-fluorothioacrolein (**15**) was obtained in 60% yield, in accord with the proposed mechanism for intramolecular conversion of allicin to thioacrolein and 2-propenesulfenic acid (Scheme 1) [1,2]. It is assumed that the second product in decomposition of **12**, 2-fluoro-2-propenesulfenic acid (**14**), self-condenses back to **12**.

Treatment of **9** with cysteine in NH₄OH afforded fluorodeoxyalliin (**13**; *S*-2-fluoro-2-propenyl-L-cysteine) in 73% yield. After crystallization **13** could be characterized by X-ray crystallography as the pure enantiomer shown in Figure 1. Structural data is given in Table 1. Two molecules co-crystallized in the structure; they are just slightly different in bond dimensions. Oxidation of an aqueous solution of **13** (30% H₂O₂) gave fluoroalliin (**22**; *S*-2-fluoro-2-propenyl-L-cysteine *S*-oxide; 82% yield). When **22** was treated with powdered fresh garlic, the presence of small amounts of **12** and isomers of mono-fluoroallicin **23** along with major amounts of allicin **4** was suggested by DART-MS analysis; the presence of **12** and **23** was also consistent with the results from ¹⁹F-NMR spectroscopy.

When a concentrated solution of **12** in 1,1,1,3,3,3-hexafluoro-2-propanol was kept at room temperature for 16 h it was converted to a 1:1 mixture of **12** and trifluoroajoene **18** ((*E,Z*)-1-(2-fluoro-3-((2-fluoroallyl)sulfinyl)prop-1-en-1-yl)-2-(2-fluoroallyl)disulfane) in 59% yield, based on

converted **12**. The choice of 1,1,1,3,3,3-hexafluoro-2-propanol follows from the observation that partial conversion of **12** to a mixture of **16–18** occurred in isopropanol, and the belief that the higher acidity of 1,1,1,3,3,3-hexafluoro-2-propanol would favor formation of **18**. When the same reaction was conducted at 60 °C, a mixture of **12**, **16** and **18** was formed, suggesting that heat favors formation of **16**. While **18** could be characterized as a mixture with **12** by NMR and liquid chromatography-high resolution mass spectrometry, separation of **12** and **18** was not possible with the chromatographic methods employed, unfortunately precluding biological studies of **18**.

Treatment of disulfide **11** with liquefied elemental sulfur at its melting point of 120 °C for 1 h, as described previously for **4** [23], afforded polysulfane mixture **21** with 4–15 sulfur atoms, with compounds containing 4–6 sulfur atoms predominating. A proposed mechanism, initiated by [2,3]-sigmatropic rearrangement of disulfide **11** (Scheme 3), is consistent with computational studies showing that fluorine substitution on the 2-position of the allyl group has little effect on rearrangement to **11a** [24]. Analysis of the complex polysulfane mixture was performed by ultra-performance liquid chromatography (UPLC) silver coordination ion spray mass spectrometry (Ag^+)CIS-MS (Figure 2) as well as by ^{19}F NMR and DART-MS techniques, as described more fully in the experimental section and elsewhere [23].

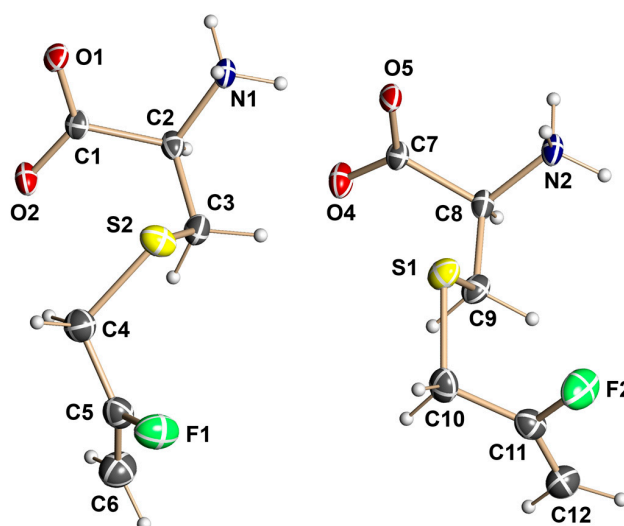
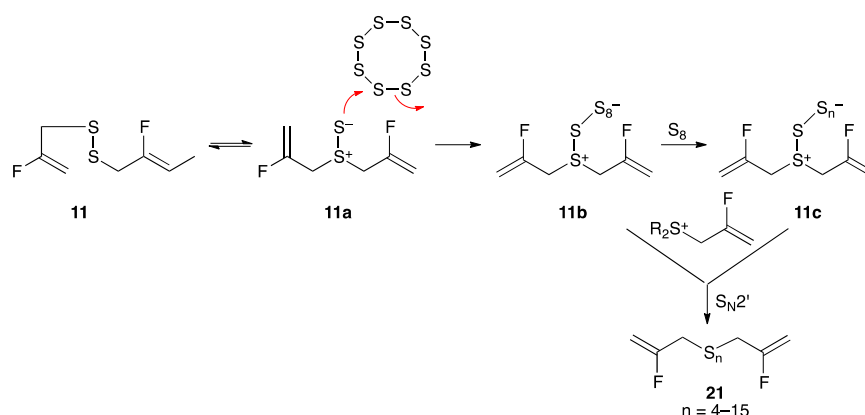


Figure 1. Molecular structure of the L-enantiomer of fluorodeoxyalliin (**13**, S-2-fluoro-2-propenyl-L-cysteine); non-hydrogen atoms are represented by thermal ellipsoids at the 50% probability level.



Scheme 3. Conversion of disulfide **11** to polysulfane mixture **21** through condensation with molten sulfur. Several equivalents of S_8 can react, losing different numbers of sulfur atom groupings, followed by $\text{S}_{\text{N}}2'$ reaction with 2-fluoroallyl sulfonium species giving polysulfane mixture **21**.

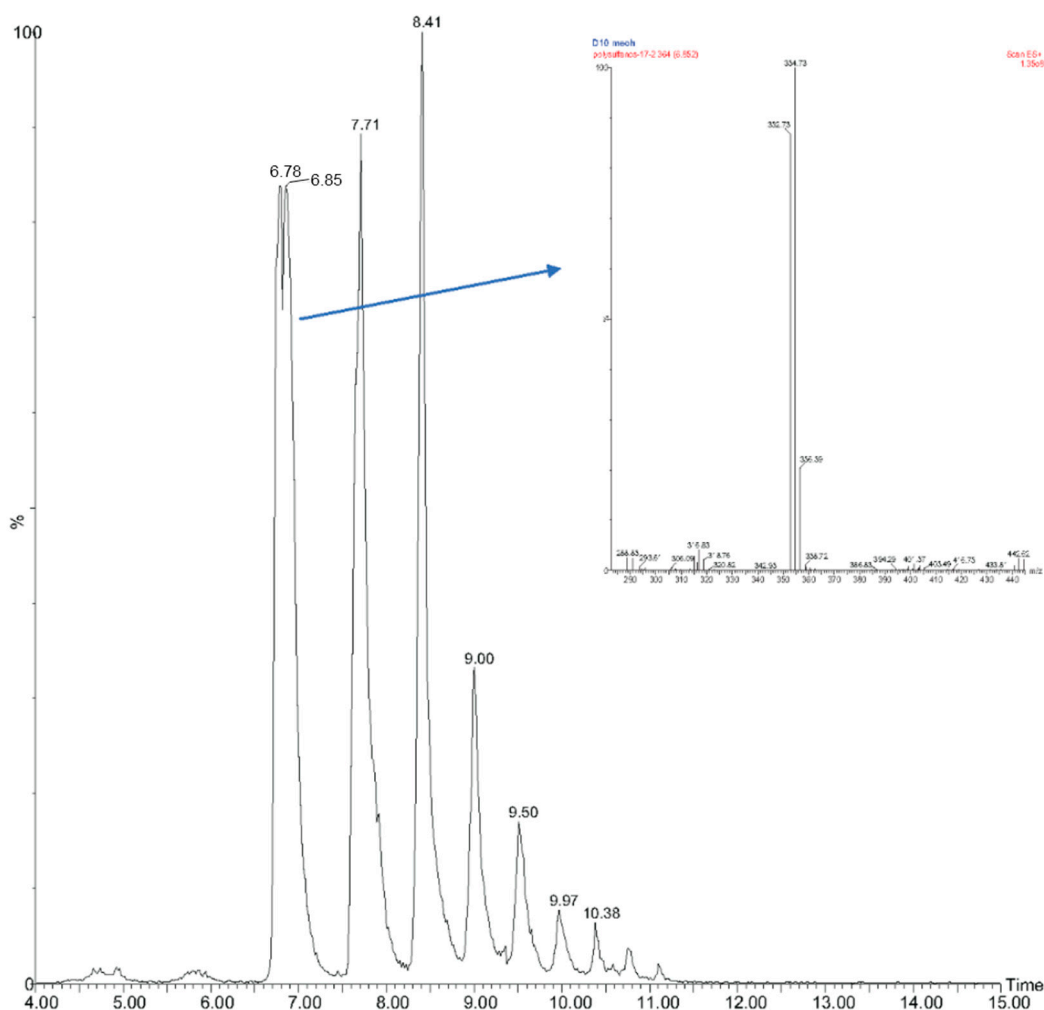


Figure 2. UPLC (Ag^+)–CIS–MS selective ion chromatogram of polysulfane mixture **21**, with 4 to 15 sulfur atoms: $\text{C}_6\text{H}_8\text{F}_2\text{S}_4\text{-}^{107}\text{Ag}$ complex, m/z 352.7, 6.78/6.85 min (split peak due to column issues); $\text{C}_6\text{H}_8\text{F}_2\text{S}_5\text{-}^{107}\text{Ag}$ complex, m/z 384.7, 7.71 min; $\text{C}_6\text{H}_8\text{F}_2\text{S}_6\text{-}^{107}\text{Ag}$ complex, m/z 416.7, 8.41 min; $\text{C}_6\text{H}_8\text{F}_2\text{S}_7\text{-}^{107}\text{Ag}$ complex, m/z 448.7, 9.00 min; $\text{C}_6\text{H}_8\text{F}_2\text{S}_8\text{-}^{107}\text{Ag}$ complex, m/z 480.7, 9.50 min; $\text{C}_6\text{H}_8\text{F}_2\text{S}_9\text{-}^{107}\text{Ag}$ complex, m/z 512.6, 9.97 min; $\text{C}_6\text{H}_8\text{F}_2\text{S}_{10}\text{-}^{107}\text{Ag}$ complex, m/z 544.5, 10.38 min; $\text{C}_6\text{H}_8\text{F}_2\text{S}_{11}\text{-}^{107}\text{Ag}$ complex, m/z 576.4, 10.7 min; and $\text{C}_6\text{H}_8\text{F}_2\text{S}_{12}\text{-}^{107}\text{Ag}$ complex, m/z 608.4, 11.1 min. With additional signal amplification, the following low abundance complexes could also be seen: $\text{C}_6\text{H}_8\text{F}_2\text{S}_{13}\text{-}^{107}\text{Ag}$ complex, m/z 640.3, 11.43 min; $\text{C}_6\text{H}_8\text{F}_2\text{S}_{14}\text{-}^{107}\text{Ag}$ complex, m/z 672.3, 11.73 min; $\text{C}_6\text{H}_8\text{F}_2\text{S}_{15}\text{-}^{107}\text{Ag}$ complex, m/z 704.2, 12.05 min. The insert shows molecular ions m/z 352.73 and 354.73 corresponding to $\text{C}_6\text{H}_8\text{F}_2\text{S}_4\text{-}^{107}\text{Ag}$ and $\text{C}_6\text{H}_8\text{F}_2\text{S}_4\text{-}^{109}\text{Ag}$. The chromatogram selecting for $\text{C}_6\text{H}_8\text{F}_2\text{S}_n\text{-}^{109}\text{Ag}$ complexes was very similar.

All new compounds were fully characterized by spectroscopic methods, either as pure compounds, or in the case of **18** mixed with **12**, **19** mixed with **20**, and **21**, as mixtures. While synthesis of fluorine-substituted analogs of garlic-derived organosulfur compounds in Scheme 1 is straightforward, their accessibility is limited by the high cost of starting material **9**. While **12** and **18** are chiral due to the sulfinyl group, thiosulfonates such as **12** are stereochemically labile [1], so no effort was made to synthesize enantiomerically pure material.

Table 1. Selected bond distances (Å) and angles (deg.) in **13**. Atom labeling corresponds to that in Figure 1.

Bond Lengths					
S(1)-C(10)	1.806(3)	C(10)-C(11)	1.472(5)	F(1)-C(5)	1.360(4)
S(1)-C(9)	1.812(3)	C(9)-C(8)	1.512(5)	C(1)-C(2)	1.524(4)
O(5)-C(7)	1.242(4)	C(11)-C(12)	1.287(5)	C(5)-C(6)	1.286(5)
O(4)-C(7)	1.238(4)	S(2)-C(4)	1.803(4)	C(5)-C(4)	1.477(5)
N(2)-C(8)	1.479(4)	S(2)-C(3)	1.815(3)	C(2)-N(1)	1.488(4)
F(2)-C(11)	1.362(4)	O(1)-C(1)	1.242(4)	C(2)-C(3)	1.510(4)
C(7)-C(8)	1.525(4)	O(2)-C(1)	1.247(4)		
Angles					
C(4)-S(2)-C(3)	100.4(2)	C(6)-C(5)-F(1)	119.4(3)	N(1)-C(2)-C(1)	109.6(3)
O(1)-C(1)-O(2)	125.8(3)	C(6)-C(5)-C(4)	129.0(4)	C(3)-C(2)-C(1)	112.4(3)
O(1)-C(1)-C(2)	118.5(3)	F(1)-C(5)-C(4)	111.5(3)	C(2)-C(3)-S(2)	113.4(2)
O(2)-C(1)-C(2)	115.7(3)	N(1)-C(2)-C(3)	110.8(3)	C(5)-C(4)-S(2)	113.4(3)

2.2. Biological Studies of Fluorinated Analogues of Garlic-Derived Organosulfur Compounds

Since ancient times, garlic has been used worldwide as a folk medicine for prevention of coronary thrombosis, stroke, and atherosclerosis, and for treatment of infections and diseases including vascular disorders, by reducing serum cholesterol levels and increasing blood coagulation times, and for treatment of cancer, by inhibiting proliferation of cancer cells [1–8]. Here, we will compare the anti-angiogenesis and antithrombotic activity of certain fluorinated analogues of garlic-derived organosulfur compounds with their non-fluorinated counterparts.

2.2.1. Anti-Angiogenesis Efficacy of Fluorinated Compounds in the Chick Chorioallantoic Membrane (CAM) Model

Angiogenesis, the formation of new blood vessels from pre-existing capillaries and circulating endothelial precursors, plays a key role in tumor growth and metastasis as well as other physiological and pathological processes such as embryonic development, chronic inflammation, and wound healing. It is regulated by factors such as vascular endothelial growth factor (VEGF), basic fibroblast growth factor (bFGF), tumor necrosis factor- α (TNF- α), and interleukin-8 (IL-8) [25].

We found that bFGF-mediated angiogenesis as examined with the CAM model was significantly inhibited ($p < 0.001$) by allicin (**1**), ajoene (**8**), difluoroallicin **12** or *S*-2-fluoro-2-propenyl-L-cysteine (**13**), with greater inhibition ($p < 0.1$) by **12** as compared to the other organosulfur compounds tested (Figure 3). Difluoroallicin **12** was significantly ($p < 0.01$) more potent than allicin (**1**) or *S*-2-fluoro-2-propenyl-L-cysteine (**13**) in inhibiting angiogenesis-mediated by bFGF. Furthermore, bis(2-fluoroallyl)polysulfane mixture **21** demonstrated comparable anti-angiogenesis efficacy against FGF-mediated angiogenesis in the CAM model to that of ajoene (Figure 4). Representative illustrations of the anti-angiogenesis efficacy of the various organosulfur compounds against FGF are shown in Figure 5, which shows the relative qualitative images that were quantitated for $n = 6–8$ CAM per arm. Additionally, a similar pattern of anti-angiogenesis efficacy for the various organosulfur compounds was also demonstrated against VEGF in the CAM model (Figure 6). At the end of the CAM study the membrane was dissected for quantitative imaging and the effect on survival of embryos was documented. Significantly, none of the treatment arms showed any mortality of the embryos at the doses tested. To complement the above CAM model, the dorsal skinfold chamber technique [26] would be a very desirable method for future use in our anti-angiogenesis studies.

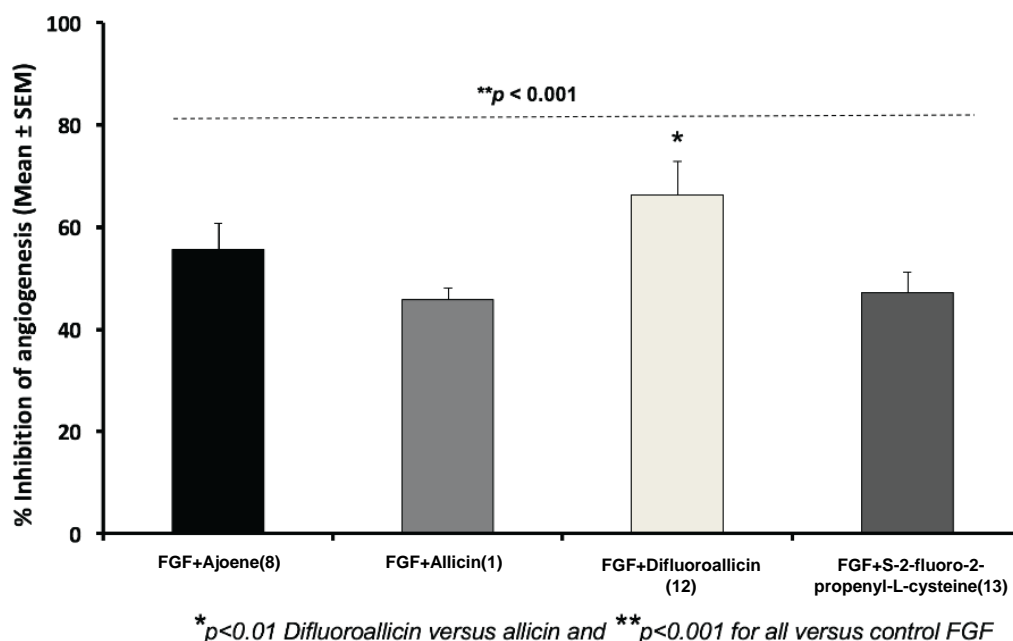


Figure 3. Inhibition of bFGF-mediated angiogenesis in the CAM model by 4 $\mu\text{g}/20 \mu\text{L}/\text{CAM}$ of ajoene (8), allicin (1), difluoroallicin 12, and S-2-fluoro-2-propenyl-L-cysteine (13); * $p < 0.01$ difluoroallicin (12) versus allicin (1) and ** $p < 0.001$ for all versus control FGF. Data showed that all organosulfur compounds tested demonstrated significant anti-angiogenesis activity, with greater efficacy for difluoroallicin 12 versus allicin (1). Data represent Mean (% inhibition of angiogenesis) \pm SEM, $n = 6\text{--}8$ CAM/group.

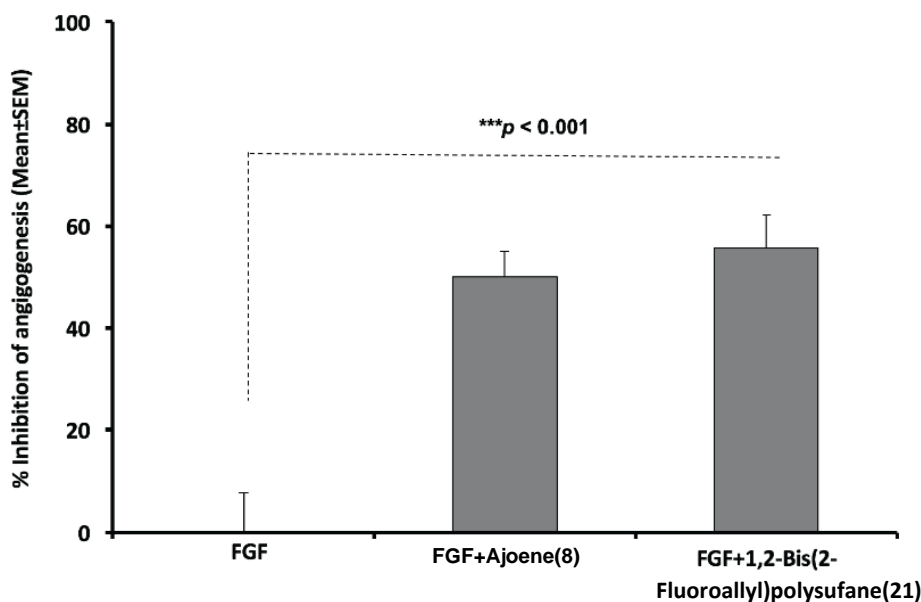


Figure 4. Anti-angiogenesis efficacy of ajoene compared with 1,2-bis(2-fluoroallyl)polysulfane mixture (21) against FGF-mediated angiogenesis in the CAM [*** $p < 0.001$] by 4 $\mu\text{g}/20 \mu\text{L}/\text{CAM}$ of ajoene (8) or 1,2-bis(2-fluoroallyl)polysulfane (21). Data showed significant (*** $p < 0.001$) and comparable anti-angiogenesis efficacy between ajoene (8) and 1,2-bis(2-fluoroallyl) polysulfane (21). Data represent Mean (% inhibition of angiogenesis) \pm SEM, $n = 8$ CAM/group.

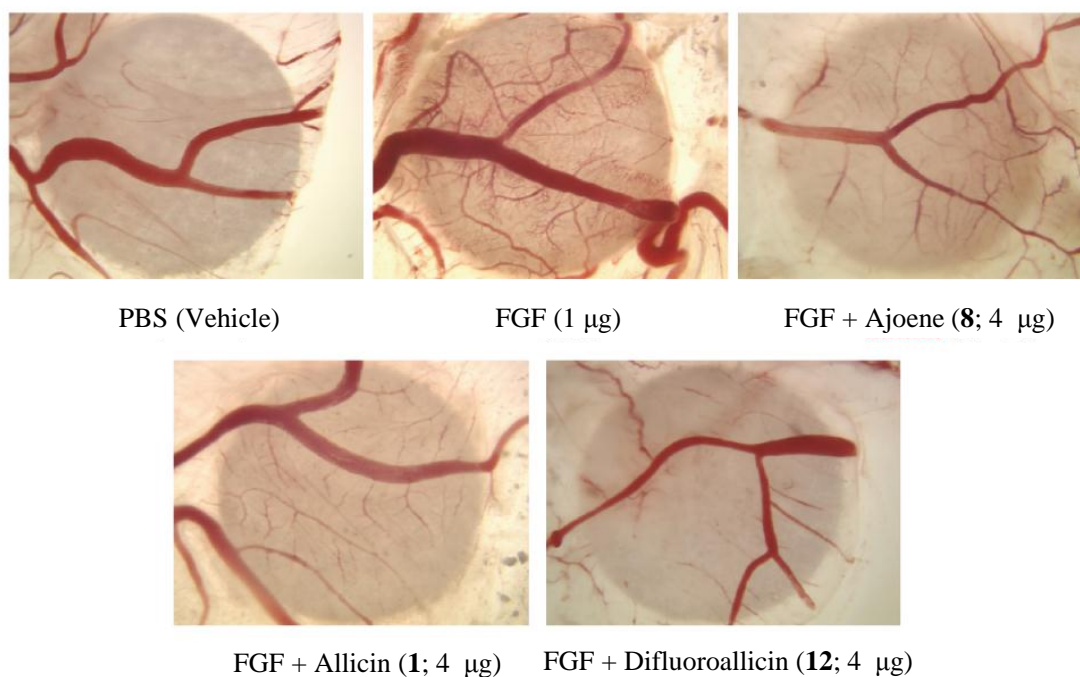


Figure 5. Representative images of CAM neovascularization induced by bFGF and inhibited by the various garlic-derived compounds including ajoene (**8**), allicin (**1**) and difluoroalliicin (**12**), each at 4 μg/20 μL/CAM. The images shown are representative single images selected for illustration of the general anti-angiogenesis efficacy of the organosulfur compounds and not for quantitative purposes.

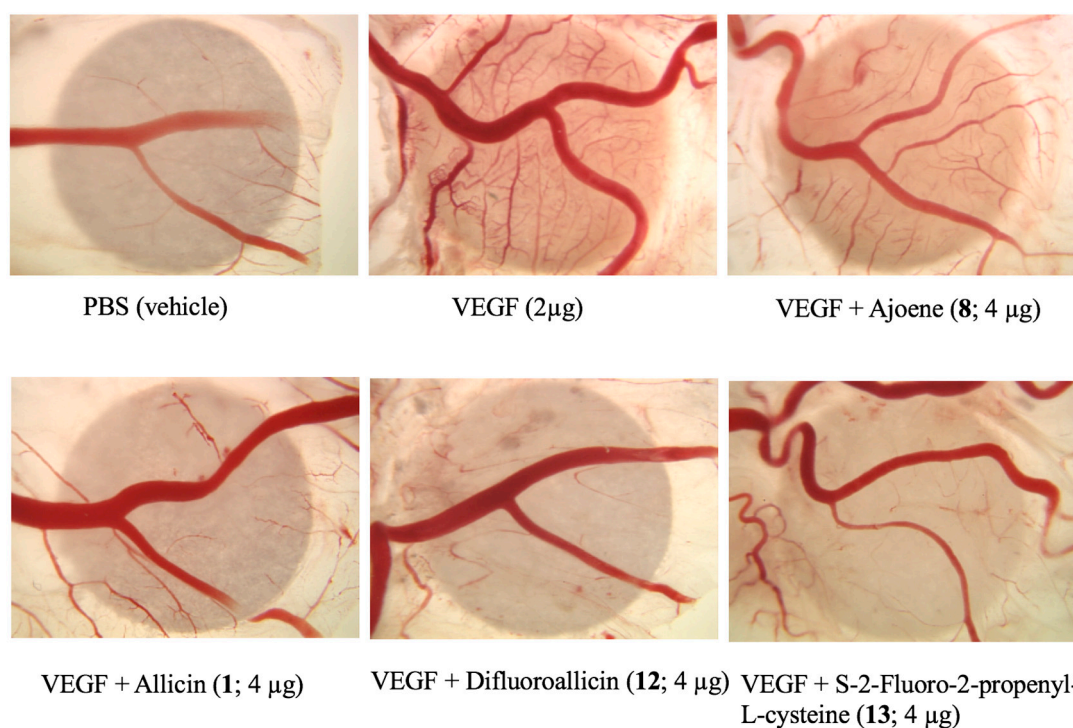


Figure 6. Representative images of CAM neovascularization induced by VEGF and inhibited by garlic-derived compounds, including ajoene (**8**), allicin (**1**), difluoroalliicin **12**, and S-2-fluoro-2-propenyl-L-cysteine (**13**), each at 4 μg/20 μL/CAM. The images shown are representative single images selected for illustration of the general anti-angiogenesis efficacy of the organosulfur compounds and not for quantitative purposes.

2.2.2. Anti-Angiogenesis Efficacy of Organosulfur Compounds in the Mouse Matrigel® Model

Difluoroallicin **12** was tested at different concentrations in the Matrigel® plug assay for its anti-angiogenesis activity. Inhibition of angiogenesis was assessed by measuring the hemoglobin level in the Matrigel® plug after 14 days of implant. Difluoroallicin **12** demonstrated a dose-dependent inhibition of angiogenesis with a maximal inhibition at 10–30 µg/plug (Figure 7).

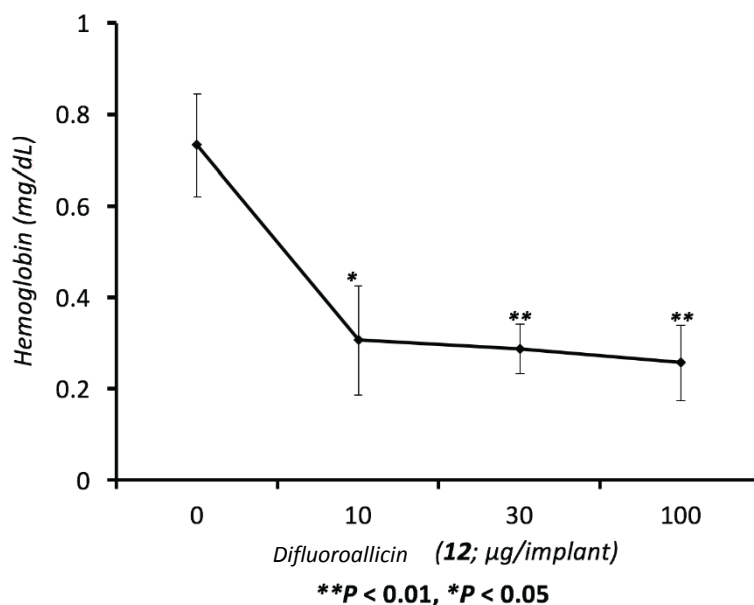


Figure 7. Dose-response inhibition of FGF-induced angiogenesis (hemoglobin, mg/dL) in FGF enriched Matrigel® with or without different doses ranging from 1–100 µg of difluoroallicin (**12**) in mice. Data represent Mean Angiogenesis index (Hemoglobin, mg/dL) ± SEM, n = 18 Matrigel® implant/group.

2.2.3. Effect of Fluorinated and Normal Organosulfur Compounds on Platelet Aggregation and Platelet/Fibrin Clot Dynamics

Antithrombotic drugs are classified as either anticoagulants or antiplatelet drugs. Anticoagulants slow down clotting, thereby reducing fibrin formation and preventing clots from forming and growing, while antiplatelet agents prevent platelets from aggregating (clumping), also preventing clots from forming and growing. The effect of various organosulfur compounds on platelet aggregation was assessed using human whole blood impedance aggregometry-induced by collagen. Allicin (**1**; 62 µM) and difluoroallicin **12** (51 µM) demonstrated the most potent inhibition of platelet aggregation ($p < 0.001$) as compared to ajoene or *S*-2-fluoro-2-propenyl-L-cysteine (**13**) (Figure 8). At these concentrations, allicin was slightly more effective compared to difluoroallicin.

For allicin, we determined platelet ATP secretion in response to collagen in human whole blood, demonstrating similar antiplatelet activity in inhibiting platelet activation by suppressing platelet ATP secretion and aggregation (Figure 9). Mayeux et al. tested the effects of allicin on platelet aggregation and showed dose dependency up to 100 µM. They also show data for cAMP levels over this concentration range [27]. Our concentrations of 10 µg/mL, equivalent to 62 µM, are comparable to the range used by Mayeux. It would be desirable to compare the activity of difluoroallicin **12** and the other fluorosulfur compounds in future studies of the type shown in Figure 9.

The effect of the various organosulfur compounds on clot strength was assessed using human whole blood thrombelastography (TEG). Difluoroallicin **12** showed the most potent inhibition of clot strength at 10–30 µg ($p < 0.001$) as compared to ajoene (**8**), allicin (**1**) or *S*-2-fluoro-2-propenyl-L-cysteine (**13**) (Figure 10). The other organosulfur compounds showed very modest effects on clot dynamics (Figure 10). Figure 11 shows representative TEG tracings of clot dynamics and kinetics, with the

most potent inhibition by difluoroallicin **12** compared to a more modest effect by allicin (**1**). The degree of inhibition of platelet aggregation for difluoroallicin **12** and allicin (**1**) is greater compared to other organosulfur compounds tested. This is in agreement with previous reports on the antiplatelet effects of allicin [22]. Distinctly greater inhibition of platelet/fibrin clot dynamics and kinetics, which translate into greater antithrombotic efficacy, was observed for difluoroallicin compared to other organosulfur compounds tested. Difluoroallicin gave a concentration-dependent inhibition of clot strength with maximal inhibition at 20–30 $\mu\text{g}/\text{mL}$ (Figure 11). We, and other investigators [21,22], reported inhibition of platelet aggregation by allicin. None of the organosulfur compounds tested showed any effects on endothelial cell (HUVEC) viability over 24 h.

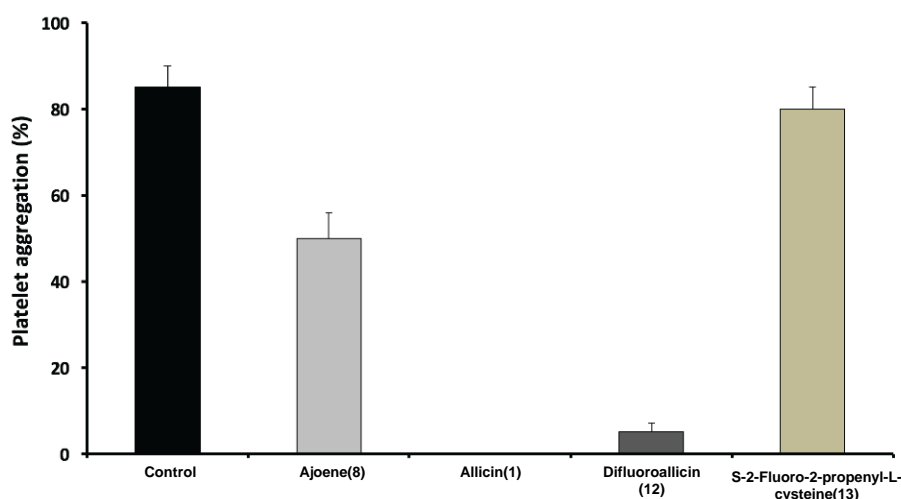


Figure 8. Effect of various garlic-derived compounds including ajoene (**8**), allicin (**1**), difluoroallicin (**12**), and S-2-fluoro-2-propenyl-L-cysteine (**13**) on human platelet aggregation at 10 $\mu\text{g}/\text{mL}$. Data represent mean platelet aggregation \pm standard deviation, $n = 3-4$.

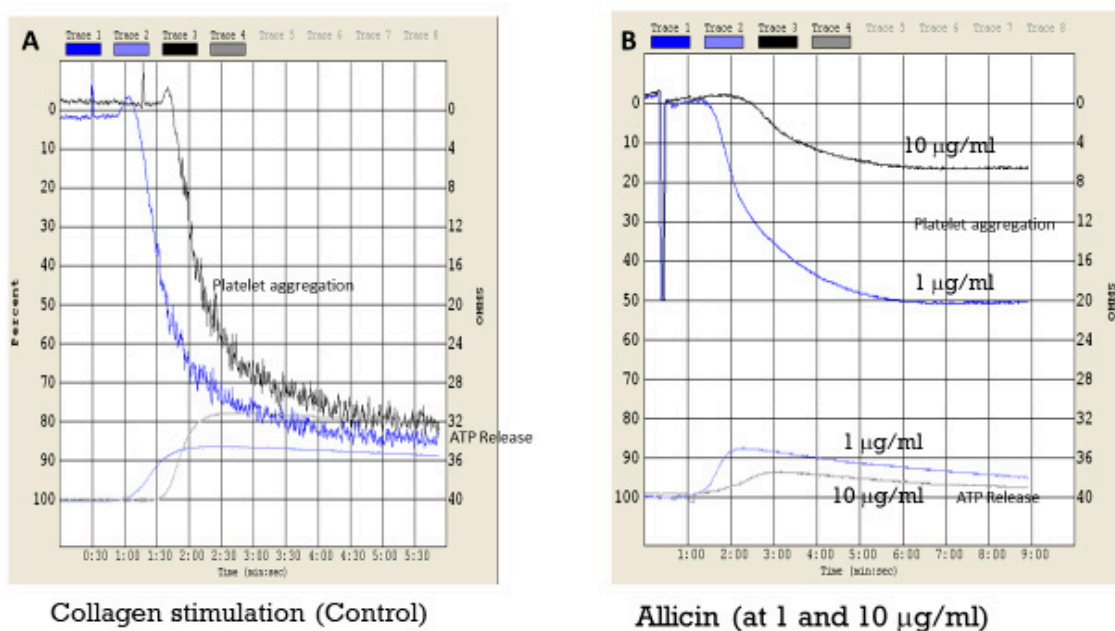


Figure 9. Representative platelet aggregation and ATP secretion in response to collagen (**A**) and collagen plus allicin at 1 and 10 $\mu\text{g}/\text{mL}$ (**B**). The representative illustration showed inhibition of both platelet aggregation and ATP secretion versus control (collagen).

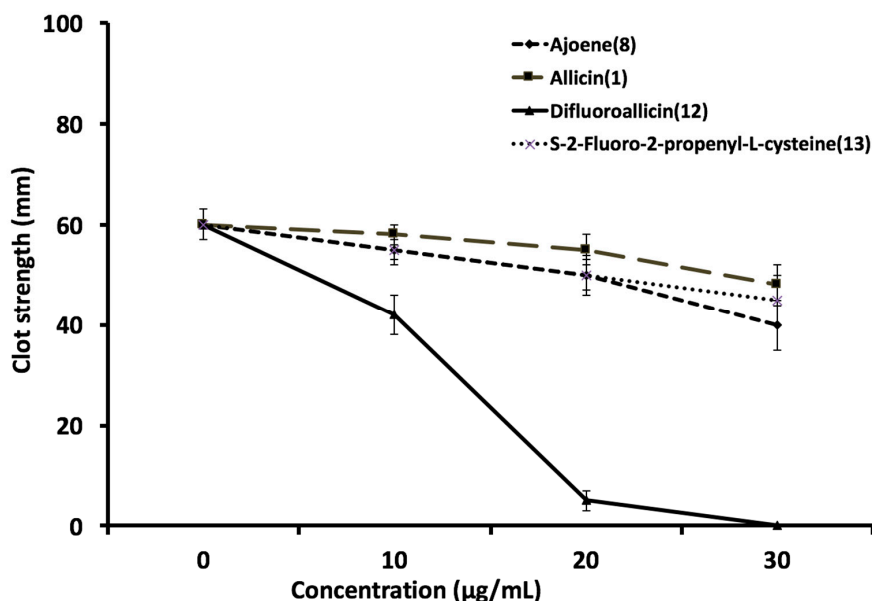


Figure 10. Effect of various garlic-derived compounds including ajoene (8), allicin (1), difluoroallicin (12), and S-2-fluoro-2-propenyl-L-cysteine (13) on clot strength in human blood using thrombelastography at different amount. Data represent mean clot strength (MA, mm) ± standard deviation, n = 4.

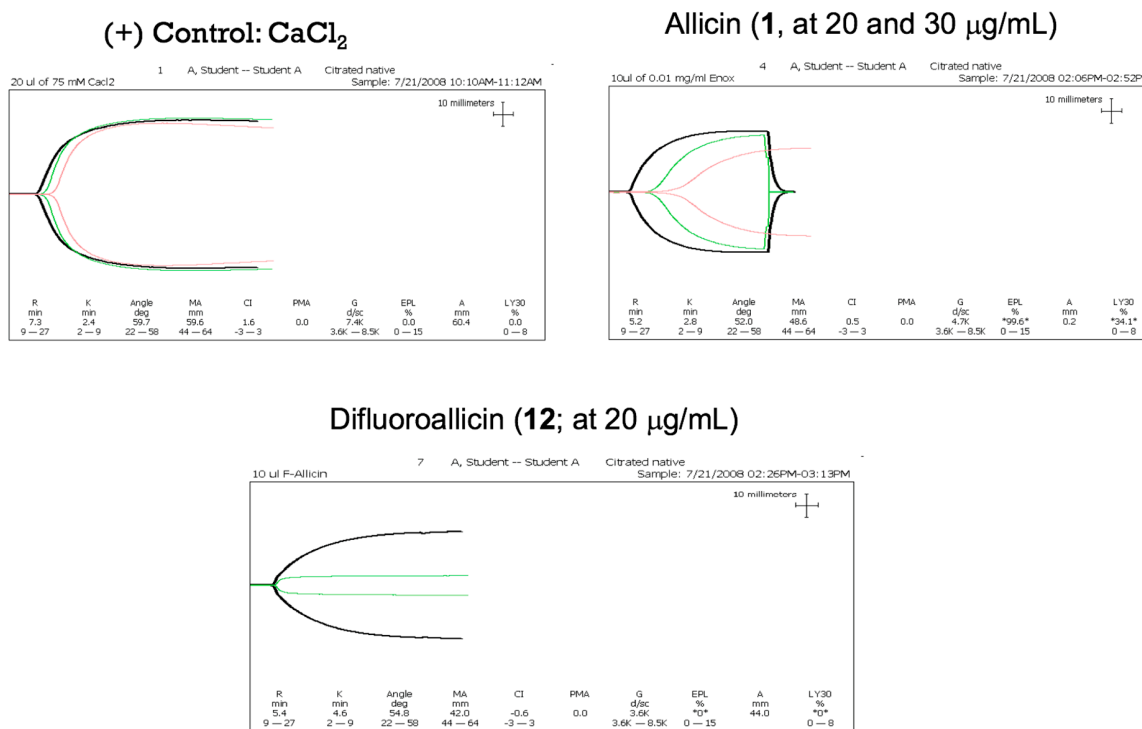


Figure 11. Representative tracing of clot kinetic for control human blood and blood treated with either allicin (1) or difluoroallicin 12 at 20–30 µg. The clot strength is measured by the width of the tracing at the end of tracing. For the positive control, there is a large width seen, which means that effective blood coagulation occurred. Difluoroallicin 12 showed distinct and greater inhibition at 20 µg/mL concentrations compared to allicin. This can be seen in the green trace relative to the control black tracing.

While comparable *antiplatelet activity* is shown for allicin (**1**) and difluoroallicin **12** (Figure 8), greater *anticoagulant activity* (inhibition of fibrin and clot strength) is shown for **12** compared to **1** (Figures 10 and 11). This is the first report illustrating the impact of allicin on coagulation activation-mediated clot kinetics. The dose-response relationship for the different compounds tested showed a slope with different degrees of inhibition of clot strength (MA, mm), suggesting a biological effect in a concentration-dependent manner on the fibrin kinetics, versus all or none, which would imply lack of toxicity (Figures 10 and 11). These data suggest an effective anti-clotting efficacy in human whole blood. Figure 10 indicates that difluoroallicin **12** at 10 $\mu\text{g}/\text{mL}$ is in fact somewhat more effective in inhibiting clot strength than allicin (**1**) and the other compounds tested. While experiments on the effects of our new fluorinated organosulfur compounds on cells in culture would be worthwhile, based on the report that different cell lines vary in their sensitivity to allicin [28], it would not necessarily be easy to extrapolate results with cells in culture to platelets in human blood.

2.2.4. Effect of Fluorine Substitution on Biological Activity

The premise in this work was that fluorine substitution would enhance the electrophilic character of allicin and other garlic-derived organosulfur compounds, which in turn would enhance their reactivity toward biological thiol groups, considered to be the defining feature of their biological activity [13–15]. While the modest, but significant, enhanced antithrombotic potency of difluoroallicin **12** compared to allicin (**1**) is in line with our expectations, the enhanced potency may also reflect changes in lipophilicity and membrane fluidity [29] associated with fluorine substitution. The anti-angiogenesis activity of 1,2-bis(2-fluoroallyl)polysulfane (**21**) is notable. Because **21** is a mixture, it would be worthwhile examining the biological activity of individual 1,2-bis(2-fluoroallyl)polysulfanes, such as the disulfide (**11**) and tetrasulfide (**21**, $n = 4$), among others.

3. Materials and Methods

3.1. General Procedures

NMR spectra were recorded in CDCl_3 , unless otherwise indicated, on a 400 Ultrashield, spectrometer (Bruker, Billerica, MA, USA) operating at 400 MHz for proton, 100 MHz for carbon, and or a Bruker 600 Avance III HD with QCI Cryoprobe operating at 600 MHz for proton, 125 MHz for carbon and 376.5 MHz for ^{19}F . The chemical shifts (δ) are indicated in ppm downfield from tetramethylsilane, with the internal standard being the residual CHCl_3 (δ 7.27 ppm for proton and δ 77.23 for carbon spectra). ^{19}F -NMR chemical shifts were relative to CFCl_3 at δ 0.00 ppm. Infrared spectra of the neat compounds were recorded on a UATR 2 FTIR (Perkin Elmer, Boston, MA USA). GC-MS were obtained using the Hewlett Packard 6890 GC and a 5972A selective mass detector (Agilent Technologies, Inc., Santa Clara, CA, USA). A DART-AccuTOF (JEOL USA, Inc., Peabody, MA, USA) time-of-flight mass spectrometer operating in positive or negative ion mode was employed with a polyethylene glycol spectrum as reference standard for exact mass measurements (PEG average molecular weight: 600). The atmospheric pressure interface was typically operated at the following potentials: orifice 1 = 15 V; orifice 2 = 5 V; ring lens = 3 V. The RF ion guide voltage was generally set to 800 V to allow detection of ions greater than m/z 80. The DART ion source was operated with helium gas at 200 $^\circ\text{C}$, and a grid voltage = 530. 3-Chloro-2-fluoroprop-1-ene (**9**) was obtained from Synquest Laboratories (Alachua, FL, USA). Selected ^1H -, ^{13}C - and ^{19}F -NMR and DART-MS data for new compounds are available in the Supporting Materials.

3.2. Synthesis of Fluorinated Garlic Organosulfur Compounds

S-(2-Fluoroallyl)ethanethioate (**10**). Potassium thioacetate (6.58 g, 57.6 mmol, 1.1 equiv.) was added to a solution of 3-chloro-2-fluoroprop-1-ene (**9**; 5 g, 53.2 mmol) in THF (150 mL). The mixture was stirred overnight to give an orange-yellow solution with a white precipitate. The solution was filtered through a silica gel pad and then concentrated in vacuo to yield the title compound (**10**; 3.23 g, 23.4 mmol, 44%)

as a yellow liquid; $^1\text{H-NMR}$ (600 MHz, CDCl_3) δ 4.53 (dd, $^3J_{\text{HF}} = 43.9$ Hz, $^2J_{\text{HH}} = 3.06$ Hz, $\text{CF}=\text{CHH}$, 1H), 4.48 (dd, $^3J_{\text{HF}} = 75.9$ Hz, $^2J_{\text{HH}} = 3.06$ Hz, $\text{CF}=\text{CHH}$, 1H), 3.58 (d, $^3J_{\text{HF}} = 17.3$ Hz, CH_2 , 2H), 2.20 (s, CH_3 , 3H); $^{13}\text{C-NMR}$ (100 MHz, CDCl_3) δ 193.7 (s), 161.5 (d, $^1J_{\text{CF}} = 257.0$ Hz), 92.6 (d, $^2J_{\text{CF}} = 19$ Hz), 30.2 (s), 29.6 (d, $^2J_{\text{CF}} = 31.3$ Hz); $^{19}\text{F-NMR}$ (376.5 MHz, CDCl_3) δ -98.3 to -98.2 (m); IR: ν_{max} 2981, 1697, 1673, 1275, 1132, 1105, 944, 857, 846, 624 cm^{-1} ; HRMS (ESI) exact mass calculated for $[\text{M} + \text{H}]^+$ ($\text{C}_5\text{H}_8\text{OFS}$) requires m/z 135.0279, found m/z 135.0290.

1,2-Bis(2-fluoroallyl)disulfane (11). Sodium chips (0.267 g, 11.63 mmol, 1.07 equiv.) were added to anhydrous methanol (100 mL) at 0°C . The mixture was stirred until the sodium disappeared completely. *S*-(2-Fluoro-2-propenyl)ethanethioate (**10**; 1.5 g, 10.87 mmol) was added at 0°C followed by iodine (1.407 g, 11.09 mmol, 1.02 equiv.) after 2 h. The mixture was stirred for 30 min and then concentrated in vacuo and purified by silica gel column chromatography (hexane) to give the title compound (**11**; 0.46 g, 2.53 mmol, 23%) as a yellow liquid; $^1\text{H-NMR}$ (600 MHz, CDCl_3) δ 4.66 (dd, $^3J_{\text{HF}} = 96.5$ Hz, $^2J_{\text{HH}} = 3$ Hz, $\text{CF}=\text{CHH}$, 1H), 4.63 (dd, $^3J_{\text{HF}} = 107$ Hz, $^2J_{\text{HH}} = 3$ Hz, $\text{CF}=\text{CHH}$, 1H), 3.42 (d, $^3J_{\text{HF}} = 18.9$ Hz, CH_2 , 2H); $^{13}\text{C-NMR}$ (100 MHz, CDCl_3) δ 161.6 (d, $^1J_{\text{CF}} = 252.0$ Hz), 94.1 (d, $^2J_{\text{CF}} = 19.0$ Hz), 39.9 (d, $^2J_{\text{CF}} = 30.2$ Hz); $^{19}\text{F-NMR}$ (376.5 MHz, CDCl_3) δ -100.57 to -100.30 (m, 2F); IR: ν_{max} 2919, 1668, 1271, 1133, 946, 891, 855, 841, 732 cm^{-1} ; HRMS (ESI) exact mass calculated for $[\text{M} + \text{H}]^+$ ($\text{C}_6\text{H}_9\text{F}_2\text{S}_2$) requires m/z 183.0114, found m/z 183.0124. In other runs, higher yields (38%) were obtained.

Difluoroallicin (12; S-(2-Fluoroallyl) 2-fluoroprop-2-ene-1-sulfinothioate). A 32% peracetic acid/acetic acid solution (0.58 g, 2.6 mmol, 1.04 equiv.) was added dropwise to a solution of bis-(2-fluoro-2-propenyl) disulfide (**11**; 0.46 g, 2.5 mmol) in chloroform (50 mL) at 0°C . The reaction mixture was vigorously stirred at 0°C for 45 min as anhydrous Na_2CO_3 (4.0 g, 37.7 mmol, 15.1 equiv.) was added in small portions. The mixture was stirred for an additional 1 h at 0°C and then filtered through a pad of Celite and anhydrous MgSO_4 . The filtrate was concentrated in vacuo at 0°C to yield the crude, water-soluble title compound **12**, which was purified by preparative TLC (4:1 pentane:diethyl ether) to give pure **12** as yellow liquid with an onion-like odor (0.21 g, 1.06 mmol, 42%); $^1\text{H-NMR}$ (600 MHz, CDCl_3) δ 4.90 (dd, $^3J_{\text{HF}} = 136$ Hz, $^2J_{\text{HH}} = 3.30$ Hz, $\text{S(O)-CH}_2\text{-CF}=\text{CHH}$, 1H), 4.85 (dd, $^3J_{\text{HF}} = 201$ Hz, $^2J_{\text{HH}} = 3.60$ Hz, $\text{S(O)-CH}_2\text{-CF}=\text{CHH}$, 1H), 4.75 (dd, $^3J_{\text{HF}} = 69.15$ Hz, $^2J_{\text{HH}} = 3.3$ Hz, $\text{S-CH}_2\text{-CF}=\text{CHH}$, 1H), 4.71 (dd, $^3J_{\text{HF}} = 97.8$ Hz, $^2J_{\text{HH}} = 3.60$ Hz, $\text{S-CH}_2\text{-CF}=\text{CHH}$, 1H), 4.00 (dd, $^4J_{\text{HF}} = 35$ Hz, $^2J_{\text{HH}} = 19.25$ Hz, S(O)-CHH , 1H), 3.99 (dd, $^4J_{\text{HF}} = 21$ Hz, $^2J_{\text{HH}} = 8.4$ Hz, S(O)-CHH , 1H), 3.86 (dd, $^4J_{\text{HF}} = 73.5$ Hz, $^2J_{\text{HH}} = 17.25$ Hz, S-CHH , 1H), 3.87 (dd, $^4J_{\text{HF}} = 42.0$ Hz, $^2J_{\text{HH}} = 17.1$ Hz, S-CHH , 1H); $^{13}\text{C-NMR}$ (100 MHz, CDCl_3) δ 32.5 (d, $^2J_{\text{CF}} = 31.0$ Hz) 58.8 (d, $^2J_{\text{CF}} = 29.0$ Hz), 94.1 (d, $^2J_{\text{CF}} = 16.9$ Hz), 98.3 (d, $^2J_{\text{CF}} = 17.9$ Hz), 155.4 (d, $^1J_{\text{CF}} = 259$ Hz) 160.5 (d, $^1J_{\text{CF}} = 161$ Hz); $^{19}\text{F-NMR}$ (376.5 MHz, CDCl_3) δ -99.65 to -99.44 (m, 1F), -94.90 to -94.62 (m, 1F); IR: ν_{max} 2917, 1669, 1407, 1272, 1081 ($\text{S}=\text{O}$), 945 cm^{-1} ; HRMS (ESI) exact mass calculated for $[\text{M} + \text{H}]^+$ ($\text{C}_6\text{H}_9\text{OF}_2\text{S}_2$) requires m/z 199.0063, found m/z 199.0080. Storage at -40°C or lower is recommended to avoid decomposition. Vacuum distillation was not attempted due to the presumed thermal sensitivity of **12**.

S-2-Fluoro-2-propenyl-L-cysteine (13; 2-Amino-3-((2-fluoroallyl)thio)propanoic acid). 3-Chloro-2-fluoroprop-1-ene (**9**) (0.94 g, 10 mmol) was added to an ice-cold solution of L-cysteine (1.21 g, 10 mmol) in ammonium hydroxide (40 mL) with vigorous stirring. The mixture was stirred at 0°C for 60 min and filtered; the filtrate was concentrated in vacuo ($<40^\circ\text{C}$) to a small volume and filtered. The solid was washed repeatedly with ethanol, dried in vacuo, and recrystallized from 2:3 water: ethanol to yield **13** as white needles (1.31 g, 7.31 mmol, 73% yield), mp $220\text{--}223^\circ\text{C}$; $^1\text{H-NMR}$ (D_2O): δ 4.75–4.51 (m, 2H), 3.90–3.87 (m, 1H), 3.32 (d, 2H, $J = 16$ Hz), 3.13–2.99 (m, 2H); $^{19}\text{F-NMR}$ (D_2O): δ -101.30 to -101.58 (m, 1F); $^{13}\text{C-NMR}$ (CCl_3): δ 172.41, 161.73, 159.21, 53.27, 31.63–31.35 (d), 31.16. Single crystals were analyzed by X-ray crystallography as described in Section 3.3 below to provide the crystal structure of the L-enantiomer shown in Figure 1.

Trifluoroajoene (18) [(E,Z)-1-(2-Fluoro-3-((2-fluoroallyl)sulfinyl)prop-1-en-1-yl)-2-(2-fluoroallyl)disulfane]. A solution of **12** (200 mg; 1.01 mmol) was dissolved in 1,1,1,3,3,3-hexafluoro-2-propanol (0.50 mL)

at room temperature. The mixture was immediately analyzed by DART-MS which showed the formation of trace amounts of trifluoroajoene **18**. The mixture was stirred at room temperature for 16 h whereupon analysis by DART-MS showed a 1:1 mixture of F-allycin and F-ajoene, with no F-dithiin present. The mixture was concentrated in vacuo to yield a faintly yellow liquid (180 mg). ^1H -, ^{13}C - and ^{19}F -NMR spectroscopy indicated a 1:1 mixture of difluoroallycin **12** and trifluoroajoene **18**, with no difluorodithiins present, corresponding to a 59% yield of **18** based on **12** converted. A small sample was stirred for 32 h but no further conversion of **12** to **18** was observed. Attempts to purify **18** by silica gel chromatography or HPLC were unsuccessful, precluding biological testing; ^1H -NMR (400 MHz, CDCl_3) **18**: δ 5.91 (d, 2H, $^3J_{\text{HF}} = 120.9$), 5.90 (s, 1H), 4.4 (m, 2H), 3.8 (m, 6H); **12** as above; ^{13}C -NMR (100 MHz, CDCl_3) **18**: δ 59.75 (d, 1C, $J = 27.70$ Hz), 60.02 (d, 1C, $J = 27.59$ Hz), 68.82 (d, 1C, $J = 33.33$ Hz), 69.32 (s, 1C), 69.81 (d, 1C, $J = 33.23$ Hz), 109.44 (d, 1C, $J = 36.08$ Hz), 108.57 (d, 1C, $J = 283.20$ Hz), 110.86 (d, 1C, $J = 247.17$ Hz), 121.75 (d, 1C, $J = 278.34$ Hz); **12** as above; ^{19}F -NMR (376.5 MHz, CDCl_3) **18**: δ -78 (s, 1F), -128 (s, 1F), -140 (s, 1F); **12** as above; HRMS (ESI) exact mass calculated for $[\text{M} + \text{H}]^+$ ($\text{C}_9\text{H}_{12}\text{F}_3\text{OS}_3$) requires m/z 289.0002, found m/z 288.9992.

5-Fluoro-3-(1-fluorovinyl)-3,4-dihydro-1,2-dithiin (16). *S*-(2-Fluoroallyl) 2-fluoroprop-2-ene-1-sulfinothioate (**12**; 50.0 mg) in CHCl_3 (1 mL) was placed in a glass tube which was sealed under vacuum and heated at 80 °C for 4.0 h. The reaction mixture was analyzed by GC-MS and the major dithiin isomer **16** was purified by flash chromatography (*n*-pentane); ^1H -NMR (400 MHz, CDCl_3) δ 3.61–2.84 (m, 2H), 3.93–3.99 (m, 1H), 4.44–4.57 (m, 1H), 4.39–4.94 (m, 1H), 6.09–6.13 (m, 1H). ^{13}C -NMR (100 MHz, CDCl_3) δ 30.3 (dd, $J = 28.0, 5.0$ Hz), 45.5 (dd, $J = 30.0, 11.5$ Hz), 93.3 (d, $J = 19.5$ Hz), 101.0 (d, $J = 27.0$ Hz), 157.0 (d, $J = 395.0$ Hz), 160.0 (d, $J = 395.0$ Hz); ^{19}F -NMR (376.5 MHz CDCl_3): δ -99.80 to -99.60 (m, 1F), -88.83 to -88.78 (m, 1F). IR: ν_{max} 2853, 1668, 1420, 1257, 1192, 1100, 928 cm^{-1} ; DART-HR-TOF-MS $[\text{M} + \text{H}]^+$ $\text{C}_6\text{H}_7\text{F}_2\text{S}_2$ found m/z 180.9958, requires m/z 180.9957.

2-Fluoroacrolein-ethyl acrylate Diels-Alder adducts: Ethyl 5-fluoro-3,4-dihydro-2H-thiopyran-2-carboxylate (19) and ethyl 5-fluoro-3,4-dihydro-2H-thiopyran-3-carboxylate (20). A mixture of difluoroallycin **12** (98.0 mg, 0.5 mmol) and ethyl acrylate (250.0 mg, 2.5 mmol) in CHCl_3 (2.5 mL) were placed in a glass tube. The tube was sealed under vacuum and heated at 100 °C for 6.0 h. The reaction mixture was analyzed by NMR and the crude material was purified by using flash chromatography (*n*-pentane/ Et_2O), affording 70:30 (**19**:**20**) mixture (56.0 mg, 60% yield). It was not possible to separate completely **19** (major) from **20** (minor) by flash chromatography. DART-HR-TOF-MS ($\text{M} + \text{H}$) $\text{C}_8\text{H}_{12}\text{FO}_2\text{S}$ found m/z 191.0538, requires m/z 191.0542. **19** (Major 70%): ^1H -NMR (400 MHz, CDCl_3) δ 5.67 (d, $J = 17.7$ Hz, 1H), 4.15–4.22 (m, 2H, overlap with **20**), 3.05–3.08 (m, 1H), 2.85–2.98 (m, 2H overlap with **20**), 2.49–2.63 (m, 2H, overlap with **20**), 1.26–1.30 (m, 3H, overlap with **20**); ^{13}C -NMR (100 MHz, CDCl_3): δ 172.0, 153.5 (d, $J = 259.7$ Hz), 97.3 (d, $J = 27.5$ Hz), 61.2, 40.7 (m, overlap with **20**), 27.2 (m, overlap with **20**), 26.4, 14.0 (overlap with **20**); ^{19}F -NMR (376.5 MHz CDCl_3): δ -96.26 to -96.21 (m). **20** (Minor 30%): ^1H -NMR (400 MHz, CDCl_3) δ 5.61 (d, $J = 17.7$ Hz, 1H), 4.15–4.22 (m, 2H, overlap with **19**), 3.35–3.43 (m, 1H), 2.85–2.98 (m, 2H), 2.49–2.63 (m, 2H, overlap with **19**), 1.26–1.30 (m, 3H, overlap with **19**); ^{13}C -NMR (100 MHz, CDCl_3) δ 170.4, 151.4 (d, $J = 259.7$ Hz), 95.7 (d, $J = 27.5$ Hz), 61.6, 40.6 (m, overlap with **19**), 27.2 (m, overlap with **19**), 23.4, 14.0 (overlap with **19**); ^{19}F -NMR (376.5 MHz CDCl_3): δ -96.09 to -96.04 (m).

Bis(2-fluoroallyl) polysulfane mixture (21). A 10 mL round-bottomed flask containing sublimed sulfur (S_8 , 0.256 g, 1.0 mmol) was placed in an oil bath pre-heated to 120 °C. When the sulfur had completely melted to a clear, straw-colored liquid, disulfide **11** (0.182 g, 1.0 mmol) was added all at once to the magnetically stirred liquid. After 30 min, the initial two-layer liquid mixture became a clear, homogeneous solution. Samples were withdrawn from the reaction mixture for analysis at various time points, e.g., 30 min, 1 h, 2 h, 4 h and 5 h. The withdrawn samples were dissolved in CDCl_3 permitting both NMR and reversed phase HPLC analysis to be performed on the same sample. For the 2 h sample, disulfide **11** eluted at 2.65 min, S_8 eluted between the heptasulfide and octasulfide at 22.2 min, and the highest polysulfane seen, eluting at 159 min, had a chain of 26 sulfur atoms.

By UPLC-(Ag⁺)-CIS-MS, chains containing up to 15 sulfur atoms could be characterized as their ¹⁰⁷Ag and ¹⁰⁹Ag adducts (see supporting information and discussion elsewhere [23]). ¹H-NMR spectroscopic analysis after 30 min shows the CH₂ proton signals as doublets centered at δ 3.39 [area 0.35, S2], 3.52 [area 0.08, S3], 3.61 [area 0.08, S4], 3.63 [area 0.16, S5], 3.64 [area 0.50, ≥S6]; after 5 h ¹H-NMR spectroscopic analysis shows 3.39 [area 0.06 S2], 3.52 [area 0.08 S3], and 3.64 [area 0.95, ≥S6]. After 1.25 h, ¹⁹F-NMR (376.5 MHz CDCl₃) showed a series of multiplets centered at δ −100.3 (**11**; C₆H₈F₂S₂) and −100.0 (C₆H₈F₂S₃) down to −99.5 ppm (C₆H₈F₂S_{>5}). DART was used to obtain HRMS (ESI) exact mass data on C₆H₉F₂S_n components in a mixture examined after 1.25 h, of heating. The lighter components gave better exact mass agreement compared to the heavier components: calculated for [M + H]⁺ (**11**; C₆H₉F₂S₂) requires *m/z* 183.0114, found *m/z* 183.0117; calculated for [M + H]⁺ (C₆H₉F₂S₃) requires *m/z* 214.9835, found *m/z* 214.9835; calculated for [M + H]⁺ (C₆H₉F₂S₄) requires *m/z* 246.9555, found *m/z* 246.9563; calculated for [M + H]⁺ (C₆H₉F₂S₅) requires *m/z* 278.9276, found *m/z* 278.9242; calculated for [M + H]⁺ (C₆H₉F₂S₆) requires *m/z* 310.8997, found *m/z* 310.8985; calculated for [M + H]⁺ (C₆H₉F₂S₇) requires *m/z* 342.8717, found *m/z* 342.8808; calculated for [M + H]⁺ (C₆H₉F₂S₈) requires *m/z* 374.8438, found *m/z* 374.9639; calculated for [M + H]⁺ (C₆H₉F₂S₉) requires *m/z* 406.8159, found *m/z* 406.9403; calculated for [M + H]⁺ (C₆H₉F₂S₁₀) requires *m/z* 438.7880, found *m/z* 438.9084. UPLC-(Ag⁺)-CIS-MS analysis of (**21**) is listed in Table S2.

(+)-*S*-2-Fluoro-2-propenyl-L-cysteine *S*-oxide (**22**). *S*-2-Fluoro-2-propenyl-L-cysteine (**13**) (1.18 g, 6.59 mmol) was added to 12 mL of water with vigorous stirring until it dissolved completely. Hydrogen peroxide (30%, 2.56 g) was added to the solution which was then stirred for 45 min at RT. The water was removed under vacuum and the title compound **22** (1.04 g, 82%, 5.33 mmol) was obtained as a white powder, mp 168–171 °C; ¹H-NMR (D₂O) 5.03 (dd, 2H, *J* = 3 Hz), 4.86–4.82 (m, 2H) 4.08–3.75 (m, 2H), 3.50–3.26 (m, 2H); ¹⁹F-NMR (D₂O) −94.84 to −95.12 (m, 1F), −95.18 to −95.47 (m, 1F).

3.3. X-ray Crystallographic Structural Determination for **13**

The single crystal diffraction data for **13** was measured on a SMART APEX CCD X-ray diffractometer (Bruker, Madison, WI, USA) equipped with a graphite monochromated Mo K α radiation source (λ = 0.71073 Å) at T = 100(2) K. Data reduction and integration were performed with the Bruker software package SAINT (Version 8.38A). Data were corrected for absorption effects using the empirical methods as implemented in SADABS. Both SAINT and SADABS are part of Bruker APEX3 software package (Version 2016.9-0): Bruker AXS, 2016. The structure was solved by SHELXTL (Version 2014/5) [30] and refined by full-matrix least-squares procedures using the Bruker SHELXTL (Version 2016/6) XL refinement program version 2016/6 software package [30]. All non-hydrogen atoms (including those in disordered parts) were refined anisotropically. The H-atoms were also included at calculated positions and refined as riders, with $U_{\text{iso}}(\text{H}) = 1.2 U_{\text{eq}}(\text{C})$ and $U_{\text{iso}}(\text{H}) = 1.5 U_{\text{eq}}(\text{N})$ for ammonia groups. Crystallographic data, details of the data collection and structure refinement for all reported compounds are listed in Table S1.

3.4. Chick Chorioallantoic Membrane (CAM) Protocols

3.4.1. Growth Factor-Mediated Angiogenesis

Chick Chorioallantoic Membrane (CAM) Model of Angiogenesis

Neovascularization was examined in the CAM model, as previously described [31–33]. Briefly, ten-day old chick embryos were purchased from Spafas, Inc. (Preston, CT, USA) and incubated at 37 °C with 55% relative humidity. Two small holes were created in the shell at the air sac and on the broadside of the egg using a hypodermic needle directly over an avascular portion of the embryonic membrane identified by candling. A false air sac beneath the second hole was created by the application of negative pressure at the first hole causing the CAM to separate from the shell. A window, approximately 1.0 cm², was cut in the shell over the dropped CAM with a small crafts

grinding wheel (Dremel, Division of Emerson Electric Co., Racine, WI, USA), allowing direct access to the underlying CAM. FGF2 (1 µg/mL) or VEGF (2 µg/mL) were used as a standard pro-angiogenic agent to induce new blood vessel branches added into the CAM membrane of the 10-day old embryos. Sterile disks of #1 filter paper (Sigma Aldrich, St. Louis, MO, USA) were pre-treated with 3 mg/mL of cortisone acetate and air dried under sterile conditions. FGF-2 and VEGF were dissolved in PBS (phosphate buffered saline). FGF2 (1 µg /mL) or VEGF (2 µg /mL) treated filter disks were placed in avascular area of the membrane. The test compound was added to membrane at different concentrations using fixed 20 µL volume.

Microscopic Analysis of CAM Sections

After incubation at 37 °C with 55% relative humidity for 3 days, the CAM tissue directly beneath each filter disk was resected from control and treated CAM samples. Tissues were washed 3 times with PBS, placed in 35-mm Petri dishes (Nalge Nunc, Rochester, NY, USA) and examined under an SV6 stereomicroscope (Karl Zeiss, Thornwood, NY, USA) at 50× magnification. Digital images of CAM sections exposed to filters were collected, using a 3-CCD color video camera system (Toshiba America, New York, NY, USA), and analyzed with Image-Pro software (Media Cybernetics, Silver Spring, MD, USA). The numbers of vessel branch points contained in a circular region equal to the area of each filter disk counted. One image was counted in each CAM preparation, and findings from 6–8 CAM preparations/group were analyzed for each treatment condition.

3.4.2. Mouse Matrigel[®]-Growth Factors Implant Angiogenesis Model

The model is as previously described [33], and was performed in accordance with institutional guidelines for animal safety and welfare. Female mice C56/BL aged 5–6 weeks and body weights of 20 g were purchased from Taconic Farms (Hudson, NY, USA). Animals were maintained under specific pathogen-free conditions and housed four animals per cage, under controlled conditions of temperature (20–24 °C) and humidity (60%–70%) and a 12 h light/dark cycle. Water and food were provided ad libitum. The in vivo study was carried out in the animal facility of the Veterans Affairs (VA) Medical Center, Albany, NY, USA and the experimental protocol was approved by the VAIACUC. Mice were acclimatized for 5 days prior to the start of experiments. Matrigel[®] Matrix High Concentration with growth factors to promote the angiogenesis was used and the mix was injected four times subcutaneously at 100 µL/animal. Animals in the control group were injected just with 100-µL volumes of Matrigel[®]. The fluorinated and non-fluorinated organosulfur compound were used at three different doses (3, 10 or 30 µg / 10 µL). Animals in the treatment groups were injected with 3, 10 or 30 µg of compounds into the 100 µL Matrigel[®] and cell mix. All groups had three mice per group, with a total of 12 Matrigel[®] subcutaneous injection per group. At day 18 post plug implant, all animals were sacrificed and hemoglobin contents were quantitated using spectrophotometry.

3.4.3. Determination of Hemoglobin (Hb) Levels (Measure of Angiogenesis Index)

Matrigel[®] plug Hb content was indexed as a measure of new vascularity. Matrigel[®] plugs were placed into a 0.5 mL tube containing double distilled water and then homogenized for 5–10 min. The samples were centrifuged at 5000× g for 10 min and then the supernatants were collected. A volume of 50 µL of supernatant was mixed with 50 µL of Drabkin's reagent and the mixture was kept at room temperature for 15–30 min, at which time 100 µL was placed in a 96-well plate and absorbance measured at 540 nm with a Microplate Manager ELISA reader (BioRad Laboratories, Hercules, CA, USA). Hb concentration is expressed as mg/dL based on comparison with a standard curve.

3.4.4. Platelet Aggregation in Whole Blood (Impedance Method)

Blood was obtained from healthy human volunteers (n = 6) who were drug-free for a minimum of 2 weeks before the blood sample collection. Blood was collected in Vacutainer tubes containing

(3.2% citrate); 500 μ L of blood incubated with 393 μ L saline, 5 μ L test compounds or 5 μ L saline and then 2 μ L of the platelet agonist collagen (1–5 μ g) was added to induce platelet aggregation and ATP secretion. An electrical impedance aggregation measurement was performed on the whole-blood aggregometer, which is equipped with automated calibration and readout functions. An aliquot of whole blood (0.5 mL) was diluted with an equivalent volume of isotonic saline and incubated for 5 min at 37 °C. The impedance of each sample was monitored in sequential 1 min intervals until a stable baseline was established. After a stable baseline established, collagen and aggregation was monitored for 10 min, and the final increase in ohms over this period was displayed [34].

3.4.5. Global Coagulation Assay (Thrombelastography)

Blood Sampling

Siliconized Vacutainer tubes (Becton Dickinson, Rutherford, NJ, USA) were used to collect whole blood. To maintain a ratio of citrate to whole blood of 1:9 (*v/v*), the tubes contained 3.2% trisodium citrate. Blood samples were placed on a slow speed rocker until TEG analysis.

Thrombelastography (TEG)

A Whole Blood Coagulation Analyzer, Model 5000 Thrombelastograph (Haemoscope Corporation, Skokie, IL, USA) was used. TEG is based on the measurement of the physical viscoelastic characteristics of blood clots. An oscillating plastic cylindrical cuvette (“cup”) and a coaxially suspended stationary piston (“pin”) with a 1-mm clearance between the surfaces are used to monitor clot formation at 37 °C. Every 4.5 s, with a 1-s mid-cycle stationary period, the cup oscillates in either direction, resulting in a frequency of 0.1 Hz. A torsion wire that acts as a torque transducer suspends the pin. Fibrin fibrils link the cup to the pin during clot formation, and the rotation of the cup is transmitted to the pin via the viscoelasticity of the clot. Customized software (Haemoscope Corporation) and an IBM-compatible personal computer display the rotation. The pin’s torque is plotted as a function of time, as shown by the different TEG clot parameters [35–38].

4. Conclusions

The organosulfur compounds tested in the CAM model have anti-angiogenesis activity against either FGF or VEGF that might have impact on pathological angiogenesis-mediated disorders such as cancer and macular degeneration, among others. Additionally, difluoroallicin **12** demonstrated effective anti-platelet activity comparable to allicin (**1**), and anticoagulant activities greater than allicin and the other organosulfur compounds tested. This is the first report illustrating the impact of allicin and its homologs on the inhibition of coagulation activation-mediated clot kinetics.

The absence of embryo mortality in all treatment arms of the CAM study suggests the lack of toxicity for **1**, **8**, **12** and **13** at the doses tested. Furthermore, the dose-response relationship for **1**, **8**, **12**, and **13** shows a slope with different degrees of inhibition of clot strength, suggesting a concentration-dependent biological effect on the fibrin kinetics, which is also inconsistent with toxicity of these compounds.

The enhanced antithrombotic potency of **12** compared to **1** is in line with expectations based on enhanced electrophilic character and/or changes in lipophilicity and membrane permeability due to fluorine substitution. These anti-thrombotic activities could have significant impact on cardiovascular and inflammatory diseases, which are associated with increased thrombosis risk. Further studies on these and related compounds are warranted pending enhanced availability of precursors such as 3-chloro-2-fluoroprop-1-ene or related compounds [39]. While we encourage others to explore this area, it should be noted that 3-chloro-2-fluoroprop-1-ene and, particularly, 2-fluoro-2-propenol are toxic (LD₅₀ for skin penetration, 200 and 4 mg/kg, respectively) and therefore should be handled with great care [40–42].

X-Ray Crystallographic Data: CCDC1577315 contains the supplementary crystallographic data, which can be obtained free of charge from Cambridge Crystallographic Data Centre, www.ccdc.cam.ac.uk/data_request/cif.

Supplementary Materials: Supplementary Materials are available online. Documentation for the X-ray structure (Table S1), UPLC-(Ag⁺)-CIS-MS analysis of bis(2-fluoro-2-propenyl) polysulfanes (**21**) (Table S2), and selected ¹H-, ¹³C- and ¹⁹F-NMR and DART-MS data for new compounds are available online.

Acknowledgments: We acknowledge support from the National Science Foundation (CHE-0744578; CHE-1265679; CHE-1337594 [MRI]; CHE-1429329 [MRI]) and the University at Albany (E.B.) and the Pharmaceutical Research Institute for funding the biological studies (S.M.), and thank Alexander Filatov and Zheng Wei for performing the X-ray structural analysis and Robert Sheridan for UPLC-MS studies. We dedicate this paper with our warmest wishes to Professor E.J. Corey on his 90th birthday.

Author Contributions: E.B. and S.A.M. conceived and designed the experiments; B.B., S.G., A.V., K.W., S.S.M., K.G. and M.Y. performed the experiments and analyzed the data; E.B. and S.A.M. wrote the paper.

Conflicts of Interest: The authors declare no conflict of interest.

References

1. Block, E. *Garlic and Other Alliums: The Lore and the Science*; Royal Society of Chemistry: Cambridge, UK, 2010.
2. Block, E. *Garlic and Other Alliums: The Lore and the Science*; Chemistry Industry Press: Beijing, China, 2017. (In Chinese)
3. Reiter, J.; Levina, N.; van der Linden, M.; Gruhlke, M.; Martin, C.; Slusarenko, A. Diallylthiosulfinate (Allicin), a Volatile Antimicrobial from Garlic (*Allium Sativum*), Kills Human Lung Pathogenic Bacteria, Including MDR Strains, as a Vapor. *Molecules* **2017**, *22*, 1711. [[CrossRef](#)] [[PubMed](#)]
4. Borlinghaus, J.; Albrecht, F.; Gruhlke, M.; Nwachukwu, I.; Slusarenko, A. Allicin: Chemistry and Biological Properties. *Molecules* **2014**, *19*, 12591–12618. [[CrossRef](#)] [[PubMed](#)]
5. Mousa, A.S.; Mousa, S.A. Anti-Angiogenesis Efficacy of the Garlic Ingredient Alliin and Antioxidants: Role of Nitric Oxide and p53. *Nutr. Cancer* **2005**, *53*, 104–110. [[CrossRef](#)] [[PubMed](#)]
6. Sela, U.; Brill, A.; Kalchenko, V.; Dashevsky, O.; Hershkoviz, R. Allicin Inhibits Blood Vessel Growth and Downregulates Akt Phosphorylation and Actin Polymerization. *Nutr. Cancer* **2008**, *60*, 412–420. [[CrossRef](#)] [[PubMed](#)]
7. Mathan, S.V.; Singh, S.V.; Singh, R.P. Fighting Cancer with Phytochemicals from Allium Vegetables. *Mol. Cancer Biol.* **2017**, *1*, e1–e23.
8. Beretta, H.V.; Bannoud, F.; Insani, M.; Berli, F.; Hirscheegger, P.; Galmarini, C.R.; Cavagnaro, P.F. Relationships among Bioactive Compounds Content and the Antiplatelet and Antioxidant Activities of Six Allium Vegetable Species. *Food Technol. Biotechnol.* **2017**, *55*, 266–275. [[CrossRef](#)] [[PubMed](#)]
9. Wang, J.; Sánchez-Roselló, M.; Aceña, J.L.; del Pozo, C.; Sorochinsky, A.E.; Fustero, S.; Soloshonok, V.A.; Liu, H. Fluorine in Pharmaceutical Industry: Fluorine-Containing Drugs Introduced to the Market in the Last Decade (2001–2011). *Chem. Rev.* **2014**, *114*, 2432–2506. [[CrossRef](#)] [[PubMed](#)]
10. Hiyama, T.; Yamamoto, H. Biologically active organofluorine compounds. In *Organofluorine Compounds: Chemistry and Applications*; Yamamoto, H., Ed.; Springer: Berlin/Heidelberg, Germany, 2000; pp. 137–182.
11. Han, Z.; Czap, G.; Chiang, C.; Xu, C.; Wagner, P.J.; Wei, X.; Zhang, Y.; Wu, R.; Ho, W. Imaging the Halogen Bond in Self-Assembled Halogenbenzenes on Silver. *Science* **2017**, *358*, 206–210. [[CrossRef](#)] [[PubMed](#)]
12. Block, E.; Booker, S.J.; Flores-Penalba, S.; George, G.N.; Gundala, S.; Landgraf, B.J.; Liu, J.; Lodge, S.N.; Pushie, M.J.; Rozovsky, S.; et al. Trifluoroselenomethionine: A New Unnatural Amino Acid. *ChemBioChem* **2016**, *17*, 1738–1751. [[CrossRef](#)] [[PubMed](#)]
13. Wallock-Richards, D.; Doherty, C.J.; Doherty, L.; Clarke, D.J.; Place, M.; Govan, J.R.W.; Campopiano, D.J. Garlic Revisited: Antimicrobial Activity of Allicin-Containing Garlic Extracts against Burkholderia Cepacia Complex. *PLoS ONE* **2014**, *9*, e112726. [[CrossRef](#)] [[PubMed](#)]
14. Müller, A.; Eller, J.; Albrecht, F.; Prochnow, P.; Kuhlmann, K.; Bandow, J.E.; Slusarenko, A.J.; Leichert, L.I.O. Allicin Induces Thiol Stress in Bacteria through S-Allylmercapto Modification of Protein Cysteines. *J. Biol. Chem.* **2016**, *291*, 11477–11490. [[CrossRef](#)] [[PubMed](#)]

15. Gruhlke, M.C.H.; Schlembach, I.; Leontiev, R.; Uebachs, A.; Gollwitzer, P.U.G.; Weiss, A.; Delaunay, A.; Toledano, M.; Slusarenko, A.J. Yap1p, the Central Regulator of the *S. cerevisiae* Oxidative Stress Response, Is Activated by Allicin, a Natural Oxidant and Defence Substance of Garlic. *Free Radic. Biol. Med.* **2017**, *108*, 793–802. [[CrossRef](#)] [[PubMed](#)]
16. Guiot, J.; Ameduri, B.; Boutevin, B. Synthesis and Polymerization of Fluorinated Monomers Bearing a Reactive Lateral Group. XII. Copolymerization of Vinylidene Fluoride with 2,3,3-Trifluoroprop-2-Enol. *J. Polym. Sci. Part A Polym. Chem.* **2002**, *40*, 3634–3643. [[CrossRef](#)]
17. Wlassics, I.; Tortelli, V.; Carella, S.; Monzani, C.; Marchionni, G. Perfluoro Allyl Fluorosulfate (FAFS): A Versatile Building Block for New Fluoroallylic Compounds. *Molecules* **2011**, *16*, 6512–6540. [[CrossRef](#)] [[PubMed](#)]
18. Daniele, G.; Corral, J.; Molife, L.R.; de Bono, J.S. FGF Receptor Inhibitors: Role in Cancer Therapy. *Curr. Oncol. Rep.* **2012**, *14*, 111–119. [[CrossRef](#)] [[PubMed](#)]
19. Falanga, A.; Russo, L.; Milesi, V.; Vignoli, A. Mechanisms and Risk Factors of Thrombosis in Cancer. *Crit. Rev. Oncol. Hematol.* **2017**, *118*, 79–83. [[CrossRef](#)] [[PubMed](#)]
20. Meikle, C.K.S.; Kelly, C.A.; Garg, P.; Wuescher, L.M.; Ali, R.A.; Worth, R.G. Cancer and Thrombosis: The Platelet Perspective. *Front. Cell Dev. Biol.* **2017**, *4*, 147. [[CrossRef](#)] [[PubMed](#)]
21. Mousa, S.A. Antithrombotic Effects of Naturally Derived Products on Coagulation and Platelet Function. *Methods Mol. Biol.* **2010**, *663*, 229–240. [[PubMed](#)]
22. Chan, J.Y.-Y.; Yuen, A.C.-Y.; Chan, R.Y.-K.; Chan, S.-W. A Review of the Cardiovascular Benefits and Antioxidant Properties of Allicin. *Phyther. Res.* **2013**, *27*, 637–646. [[CrossRef](#)] [[PubMed](#)]
23. Wang, K.; Groom, M.; Sheridan, R.; Zhang, S.; Block, E. Liquid Sulfur as a Reagent: Synthesis of Polysulfanes with 20 or More Sulfur Atoms with Characterization by UPLC-(Ag⁺)-Coordination Ion Spray-MS. *J. Sulfur Chem.* **2013**, *34*, 55–66. [[CrossRef](#)]
24. Li, Z.; Wang, C.; Fu, Y.; Guo, Q.-X.; Liu, L. Substituent Effect on the Efficiency of Desulfurizative Rearrangement of Allylic Disulfides. *J. Org. Chem.* **2008**, *73*, 6127–6136. [[CrossRef](#)] [[PubMed](#)]
25. Folkman, J.; Shing, Y. Angiogenesis. *J. Biol. Chem.* **1992**, *267*, 10931–10934. [[PubMed](#)]
26. Laschke, M.; Menger, M. The Dorsal Skinfold Chamber: A Versatile Tool for Preclinical Research in Tissue Engineering and Regenerative Medicine. *Eur. Cells Mater.* **2016**, *32*, 202–215. [[CrossRef](#)] [[PubMed](#)]
27. Mayeux, P.R.; Agrawal, K.C.; Tou, J.S.; King, B.T.; Lippton, H.L.; Hyman, A.L.; Kadowitz, P.J.; McNamara, D.B. The Pharmacological Effects of Allicin, a Constituent of Garlic Oil. *Agents Actions* **1988**, *25*, 182–190. [[CrossRef](#)] [[PubMed](#)]
28. Gruhlke, M.; Nicco, C.; Batteux, F.; Slusarenko, A. The Effects of Allicin, a Reactive Sulfur Species from Garlic, on a Selection of Mammalian Cell Lines. *Antioxidants* **2016**, *6*, 1. [[CrossRef](#)] [[PubMed](#)]
29. Tsuchiya, H.; Nagayama, M. Garlic Allyl Derivatives Interact with Membrane Lipids to Modify the Membrane Fluidity. *J. Biomed. Sci.* **2008**, *15*, 653–660. [[CrossRef](#)] [[PubMed](#)]
30. Sheldrick, G.M. Crystal Structure Refinement with SHELXL. *Acta Crystallogr. Sect. C Struct. Chem.* **2015**, *71*, 3–8. [[CrossRef](#)] [[PubMed](#)]
31. Marcinkiewicz, C.; Weinreb, P.H.; Calvete, J.J.; Kisiel, D.G.; Mousa, S.A.; Tuszyński, G.P.; Lobb, R.R. Obtustatin. *Cancer Res.* **2003**, *63*, 2020–2023. [[PubMed](#)]
32. Deryugina, E.I.; Quigley, J.P. Chick embryo chorioallantoic membrane models to quantify angiogenesis induced by inflammatory and tumor cells or purified effector molecules. *Methods Enzymol.* **2008**, *444*, 21–41. [[PubMed](#)]
33. Bridoux, A.; Cui, H.; Dyskin, E.; Yalcin, M.; Mousa, S.A. Semisynthesis and Pharmacological Activities of Tetrac Analogs: Angiogenesis Modulators. *Bioorg. Med. Chem. Lett.* **2009**, *19*, 3259–3263. [[CrossRef](#)] [[PubMed](#)]
34. Mousa, S.S.; Davis, F.B.; Davis, P.J.; Mousa, S.A. Human Platelet Aggregation and Degranulation Is Induced In Vitro by L-Thyroxine, but Not by 3,5,3'-Triiodo-L-Thyronine or Diiodothyropropionic Acid (DITPA). *Clin. Appl. Thromb.* **2010**, *16*, 288–293. [[CrossRef](#)] [[PubMed](#)]
35. Mousa, S.A. In Vitro Efficacy of Different Platelet Glycoprotein IIb/IIIa Antagonists and Thrombolytics on Platelet/fibrin-Mediated Clot Dynamics in Human Whole Blood Using Thrombelastography. *Blood Coagul. Fibrinolysis* **2007**, *18*, 55–60. [[CrossRef](#)] [[PubMed](#)]

36. Mousa, S.A.; Forsythe, M.S. Comparison of the Effect of Different Platelet GPIIb/IIIa Antagonists on the Dynamics of Platelet/fibrin-Mediated Clot Strength Induced Using Thromboelastography. *Thromb. Res.* **2001**, *104*, 49–56. [[CrossRef](#)]
37. Mousa, S.A. Comparative Efficacy of Different Low-Molecular-Weight Heparins (LMWHs) and Drug Interactions with LMWH: Implications for Management of Vascular Disorders. *Semin. Thromb. Hemost.* **2000**, *26* (Suppl. 1), 39–46. [[CrossRef](#)] [[PubMed](#)]
38. Mousa, S.A.; Khurana, S.; Forsythe, M.S. Comparative in Vitro Efficacy of Different Platelet Glycoprotein IIb/IIIa Antagonists on Platelet-Mediated Clot Strength Induced by Tissue Factor with Use of Thromboelastography: Differentiation among Glycoprotein IIb/IIIa Antagonists. *Arterioscler. Thromb. Vasc. Biol.* **2000**, *20*, 1162–1167. [[CrossRef](#)] [[PubMed](#)]
39. Laue, K.W.; Haufe, G. 3-Bromo-2-Fluoropropene—A Fluorinated Building Block. 2-Fluoroallylation of Glycine and Alanine Ester Imines. *Synthesis* **1998**, *1998*, 1453–1456. [[CrossRef](#)]
40. Moore, L.O.; Henry, J.P.; Clark, J.W. Chlorination of 2-Fluoropropene. 3-Chloro-2-Fluoropropene and Some of Its Derivatives. *J. Org. Chem.* **1970**, *35*, 4201–4204. [[CrossRef](#)]
41. Tkachenko, A.N.; Radchenko, D.S.; Mykhailiuk, P.K.; Grygorenko, O.O.; Komarov, I.V. 4-Fluoro-2,4-Methanoproline. *Org. Lett.* **2009**, *11*, 5674–5676. [[CrossRef](#)] [[PubMed](#)]
42. Smyth, H.F.; Carpenter, C.P.; Well, C.S.; Pozzani, U.C.; Striegel, J.A. Range-Finding Toxicity Data: List VI. *Am. Ind. Hyg. Assoc. J.* **1962**, *23*, 95–107. [[CrossRef](#)] [[PubMed](#)]

Sample Availability: Samples of the compounds described in the text are not available from the authors.



© 2017 by the authors. Licensee MDPI, Basel, Switzerland. This article is an open access article distributed under the terms and conditions of the Creative Commons Attribution (CC BY) license (<http://creativecommons.org/licenses/by/4.0/>).